Supplementary information

for

Efficient solution-processed fluorescent OLEDs realized by removing charge trapping emission loss of BODIPY fluorochrome

Lisi Chen [a], Mei Chen [a], Yeyin Lan [a], Yongxin Chang [b], Xianfeng Qiao [c], Chunlan Tao [a]*, Xiaolong Zhao [b]*, Dongdong Qin [a]*, Yuwei Zhang [a,d]*, Baohua Zhang [a] and Li Niu [a]

[a] Center for Advanced Analytical Science, Guangzhou Key Laboratory of Sensing Materials and Devices, Guangdong Engineering Technology Research Center for Photoelectric Sensing Materials and Devices, c/o School of Chemistry and Chemical Engineering, Guangzhou University, Guangzhou 510006, China.

[b] Key Laboratory of Eco-Functional Polymer Materials, Ministry of Education, College of Chemistry and Chemical Engineering, Northwest Normal University, Lanzhou 730070, China.

c Institute of Polymer Optoelectronic Materials and Devices, Guangdong−Hong Kong−Macao Joint Laboratory of Optoelectronic and Magnetic Functional Materials, Guangdong Provincial Key Laboratory of Luminescence from Molecular Aggregates, State Key Laboratory of Luminescent Materials and Devices, South China University of Technology, Guangzhou 510640, China

[d] GDMPA Key Laboratory for Process Control and Quality Evaluation of Chiral Pharmaceuticals, Guangzhou Key Laboratory of Analytical Chemistry for Biomedicine, School of Chemistry, South China Normal University, Guangzhou 510006, China.

Note: Lisi Chen and Mei Chen contributed equally to this work.

*Corresponding Author, Email: taochl@gzhu.edu.cn (C. Tao), zhaoxl82@nwnu.edu.cn (X. Zhao), ccqindd@gzhu.edu.cn (D. Qin), ywzhang@scnu.edu.cn (Y. Zhang)

1 Experimental Section

1.1 The synthesis procedure

1.1.1 Synthesis of BDP-1

To a 250 mL round bottom flask with stir bar, 2, 4-Dimethylpyrrole (0.46 mL, 4.63 mmol) and benzaldehyde (0.24 g, 2.30 mmol) were added to dry dichloromethane (DCM) (100 mL). To this mixture, 3 drops of trifluoroacetic acid (TFA) were added, and the reaction was left to stir in an atmosphere of argon. The reaction progress was monitored by TLC until benzaldehyde was consumed. Then 2,3-dichloro-5,6-dicyano-1,4-benzoquinone (DDQ) (0.52 g, 2.29 mmol) was added, and the solution was left to stir over 30 min and followed by the drop-wise addition of trimethylamine (TEA) (3.16 mL, 23 mmol) and BF_3•Et_2O (2.90 mL, 23 mmol). After being stirred for 4 h at room temperature, the reaction mixture was poured into saturated saline and extracted with DCM (200 mL). The organic phase was washed successively with H_2O (200 mL) and brine (100 mL), dried with Na_2SO_4 and concentrated under reduced pressure. The mixture was purified by silica gel flash column chromatography (silica gel, EtOAc/petroleum ether, V:V＝1:4) yielded red crystals of BDP-1 (543 mg, 72% yield). ^{1}H NMR (600 MHz, $CDCl_3$) δ 7.51-7.46 (m, 3H), 7.28 (dd, J = 7.3, 2.1 Hz, 2H), 5.98 (s, 2H), 2.56 (s, 6H), 1.37 (s, 6H); ^{13}C NMR (150 MHz, CDCl3) δ 155.4, 143.1, 129.1, 128.9, 127.9, 121.2, 14.6, 14.3. ESI-MS calcd for $C_{19}H_{19}BF_2N_2$ $[M^+H]^+$ 323.2188, found 323.2207. HLCT purity: 99.54%.

1.1.2 Synthesis of BDP-2

Synthesis of BDP-2 was carried out in one pot reaction as the procedure in BDP-1. The mixture was purified by silica gel flash column chromatography(silica gel, EtOAc/petroleum ether, V:V＝1:4)to yield red crystals of BDP-2 (594 mg, 69% yield). ^{1}H NMR (600 MHz, CDCl3) δ 7.96 (d, J = 8.2 Hz, 1H), 7.89 (d, J = 8.1 Hz, 1H), 7.80 (d, J = 8.3 Hz, 1H), 7.59-7.55 (m, 1H), 7.52 (t, J = 7.2 Hz, 1H), 7.44 (t, J = 7.6 Hz, 1H), 7.40 (d, J = 6.9 Hz, 1H), 5.94 (s, 2H), 2.59 (s, 6H), 1.05 (s, 6H); ^{13}C NMR (150 MHz, $CDCl_3$) δ 155.6, 143.0, 140.1, 133.5, 132.4, 131.9, 131.7, 129.2, 128.1, 127.2, 126.6, 125.9, 125.7, 124.9, 121.1, 14.6, 13.8. ESI-MS calcd for $C_{23}H_{21}BF_2N_2$ $[M^+Na]^+$ 397.1665, found 397.1687. HLCT purity: 98.41%.

1.1.3 Synthesis of BDP-3

Synthesis of BDP-3 was carried out in a one pot reaction as the procedure in BDP-1. The mixture was purified by silica gel flash column chromatography(silica gel, EtOAc/petroleum ether, V:V＝1:4)to yield red crystals of BDP-3 (644 mg, 66% yield). ^{1}H NMR (600 MHz, $CDCl_3$) δ 8.57 (s, 1H), 8.03 (d, J = 8.4 Hz, 2H), 7.93-7.89 (m, 2H), 7.51-7.47 (m, 2H), 7.45-7.41 (m, 2H), 5.89 (s, 2H), 2.63 (s, 6H), 0.65 (s, 6H); ^{13}C NMR (150 MHz, $CDCl_3$) δ 155.7, 142.9, 138.9, 132.3, 131.3, 129.7, 128.3, 128.2, 126.9, 125.7, 125.1, 121.1, 77.2, 14.7, 13.3. ESI-MS calcd for $C_{27}H_{23}BF_2N_2$ $[M^+H]^+$ 425.1966, found 425.1989. HLCT purity: 98.19%.

1.2 Instruments and reagents

The ^{1}H NMR (600 MHz) spectra and the ^{13}C NMR (150 MHz) spectra were recorded at room temperature on an Agilent DD2 600 spectrometers with chemical shifts referenced to internal TMS, and chemical shifts are reported relative to the solvent residue peaks ($CDCl_3$, δ 7.26 for ^{1}H NMR, δ 77.16 for ^{13}C NMR). High-resolution mass spectra (HRMS) were obtained from Agilent 6510 Accurate-Mass Q-TOF LC/MS system. UV-Vis and fluorescent spectra were carried out on a T6 and F97pro fluorescence spectrophotometer, respectively. All the solvents used in optical experiment were analytical grade. Dry dichloromethane was obtained by refluxing in calcium hydride. Aqueous solutions were freshly prepared with twice-deionized water from a water purification system. Pre-coated silica plates for thin-layer chromatography (TLC) analysis and silica gel (mesh 200~300) for column chromatography were purchased from the Qingdao Ocean Chemicals. For X-ray single crystal structure characterization, it was measured by Rigaku Oxford Diffraction, GUI svn.r6498, CrysAlis^{Pro}) and drawn and analyzed by Mercury software.

Cary60 (Agilent) instrument was used to test the UV-vis absorption spectrum of the material, Edinburgh Fluorescence Spectrometer (FLS1000) was used to characterize the photophysics of the material, in which the steady-state spectrum of PL was excited by Xe_2 xenon lamp, and the transient spectrum was measured by the picosecond pulsed LED (PLED-365). The Φ_{PL} is measured by the built-in integrating sphere. For measurement of the orientation of emitting dipoles in emitters, a setup RSQX-01 made by the Changchun Ruoshui Technology Development Co., Ltd. was used.

The cyclic voltammetry was tested using a CHI760E Electrochemical Workstation (CH Instruments Inc.) analyzer. In the CV system, 0.1M tetrabutylammonium hexafluorophosphate (TBAPF6) was used as the electrolyte, and the material was used in ultra-dry acetonitrile solution (10^{-4}M) at the rate of 50 mV s^{-1} to measure the electrochemical properties of three typical electrodes (platinum disk as the working electrode, platinum wire as the reverse electrode, and silver wire as the reference electrode). Ferrocene/ferrocene (Fc/Fc^{+}) is the external standard compound.

In the liquid-phase diffusion method, 5 milligrams of the sample were dissolved in 1 ml of dichloromethane, and then 5 ml of petroleum ether were slowly added for single crystal growth, resulting in high-quality single crystals of BOD-2 for the subsequent single crystal test.

The surface morphology of EMLs films was measured by atomic force microscopy (AFM). The miscibility of different active materials in EMLs and the film forming property of EMLs films were evaluated. The tested film structure is ITO/PEDOT: PSS/EMLs.

1.3 OLED Device Fabrication

OLED is based on a glass substrate coated with an ITO layer as an anode, which has a resistance of 15 Ω cm^{-2}. The preparation process of the device is as follows: the ITO slide needs to be cleaned with ultrasonic wave in alcohol and deionized water respectively for 30min, then dried in an oven at 120℃ for 2h, and then treated with ultraviolet ozone for 20min. After that, the luminescent layer and the transport layer were prepared by spin coating and evaporation successively. The device structure we adopted was ITO/PEDOT: PSS/EML/TmPyPB (60 nm)/LiF (1 nm)/Al (100 nm). First, PEDOT: PSS was coated on ITO by rotating at 4000 rpm, and then annealed at 120℃ for 30min. The above steps are carried out in air, and the subsequent steps will be carried out in a glove box filled with N_2 (Brann, Shanghai, $[O_2] < 0.1$ ppm, $[H_2O] < 0.1$ ppm). A mixture of EMLs with a concentration of 10mg ml-1 in chlorobenzene was then spin coated into the PEDOT: PSS layer, followed by annealing at 80 °C for 30 min. Subsequent deposits of TmPyPB, LiF, and Al were sequentially deposited in vacuum chambers (base pressure below 5×10^{-6} mbar) (EVOVAC, Angstrom Engineering Corp., Canada). Finally, a computer-controlled current-voltage-brightness

system (FS-2000TR, Fstar) was used to test the prepared OLED. During the test, the EL spectrum was measured by the CS2000A device. OLED is not packaged, and the tests are all measured under air.

2. Additional Figures and Tables

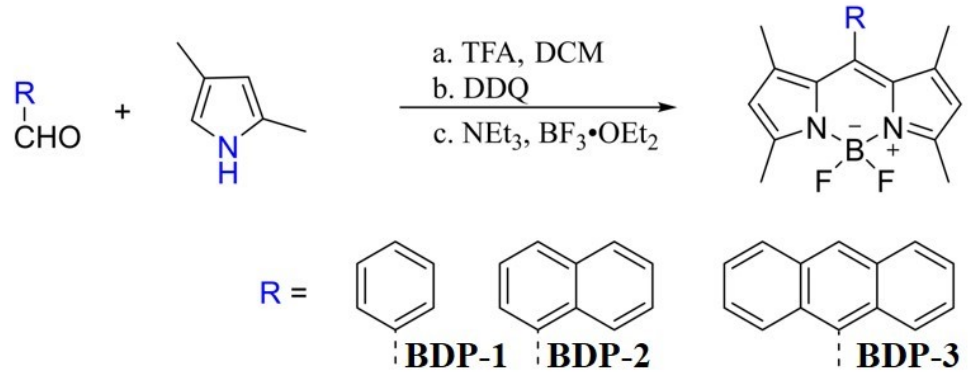

Scheme S1. Synthesis Scheme of BDP-1~3.

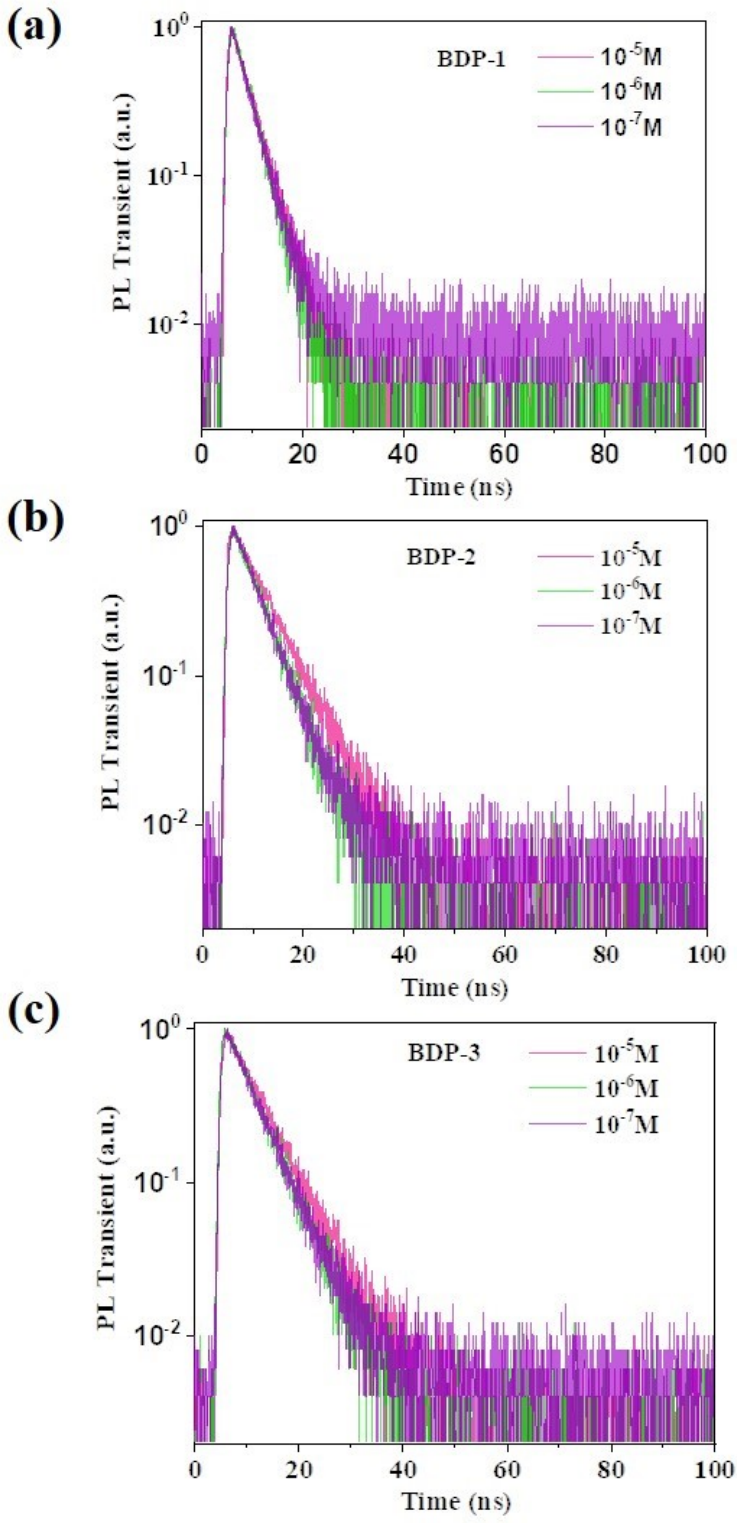

Figure S1. PL transient measurements of BDP-1, BDP-2 and BDP-3 in the concentration ranging from 10^{-5} M to 10^{-7} M, respectively.

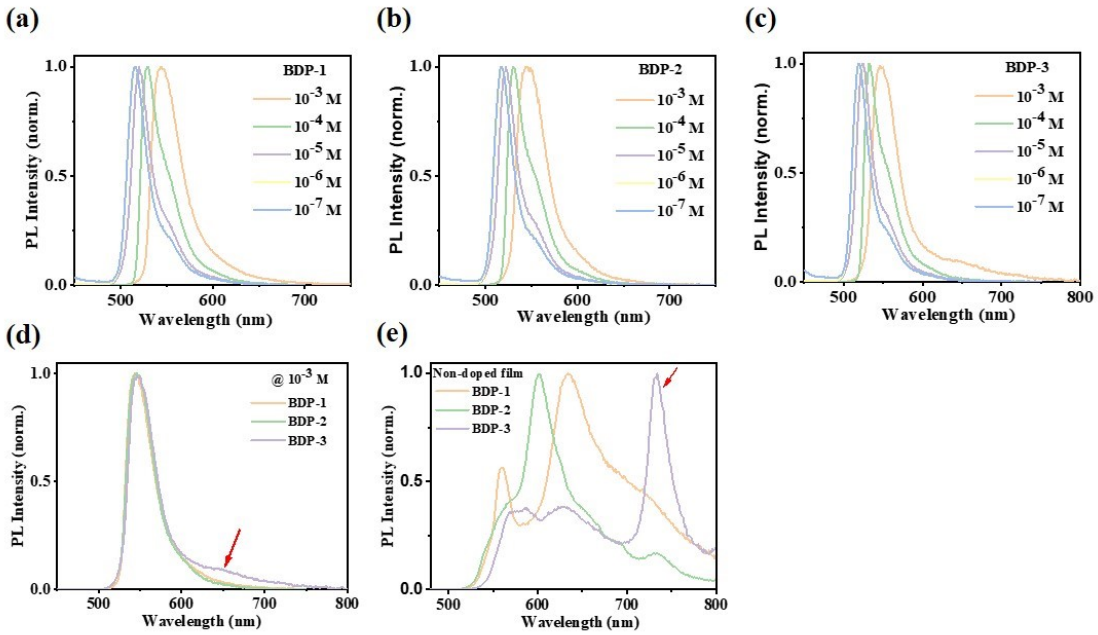

Figure S2. (a~c) PL spectra of BDP-1~3 at different concentrations in chlorobenzene. (d) PL spectra of BDP-1~3 at 10^{-3}M in chlorobenzene. (e) PL spectra of BDP-1~3 non-doped films.

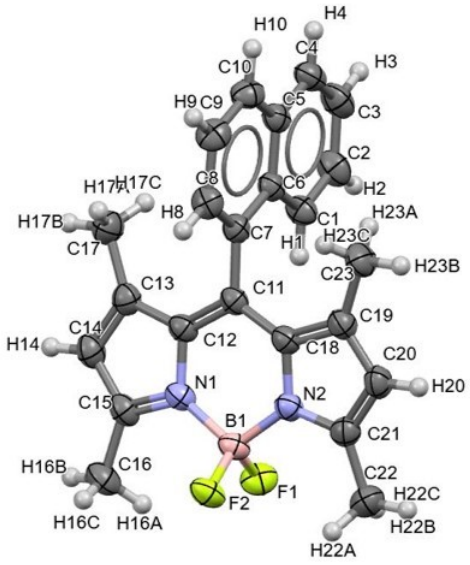

Figure S3. Crystal structure of BDP-2 (50% probability ellipsoids), in which bond types of all unknown links were guessed automatically from single crystalline data via Mercury software.

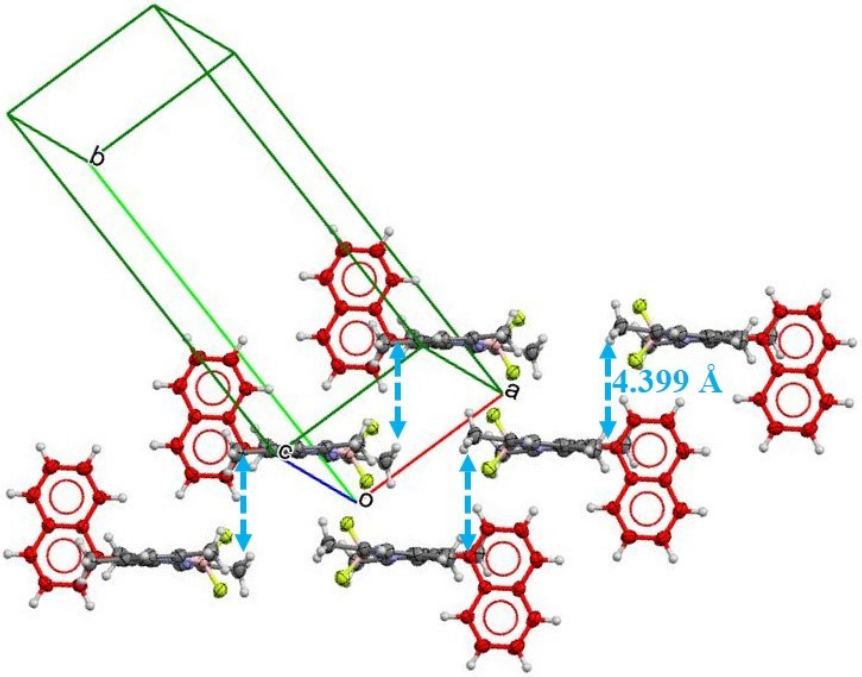

Figure S4. Molecular packing mode of BDP-2 in single crystal, in which naphthalene groups are highlighted as red colors.

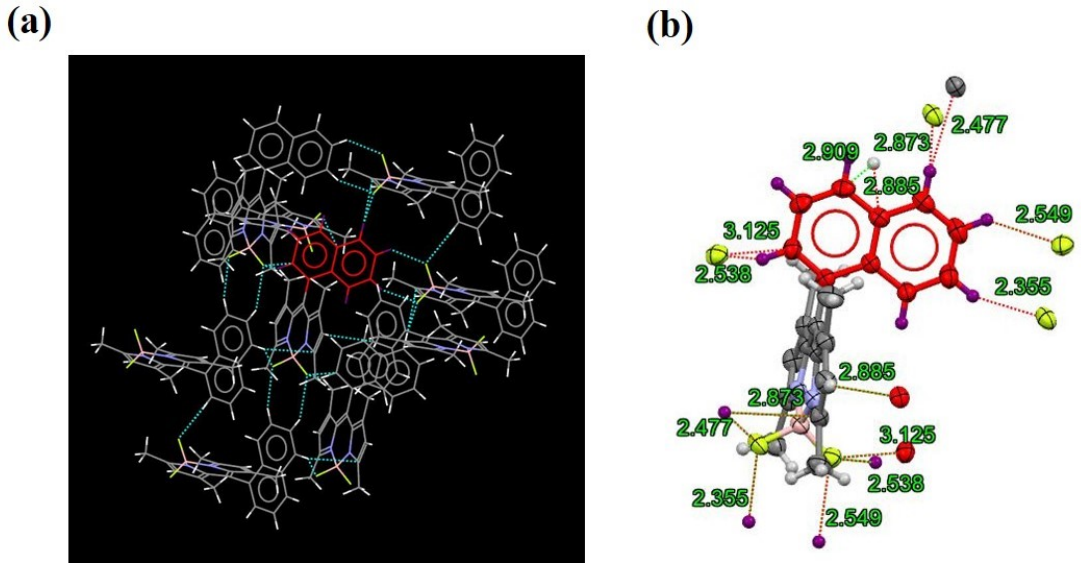

Figure S5. (a) the crystal structure of the concerned center BDP-2 molecules with the nearest neighboring eight molecules with intermolecular van der Waals (vdW) force interactions (default setting in Mercury), in which the naphthalene group of the concerned BDP-2 molecule is highlighted as red colors (styles: wireframe); (b) the illustration of one BDP-2 (styles: ellipsoid) with vdW force interactions, in which the force distances between this molecule and neighboring atoms are labelled.

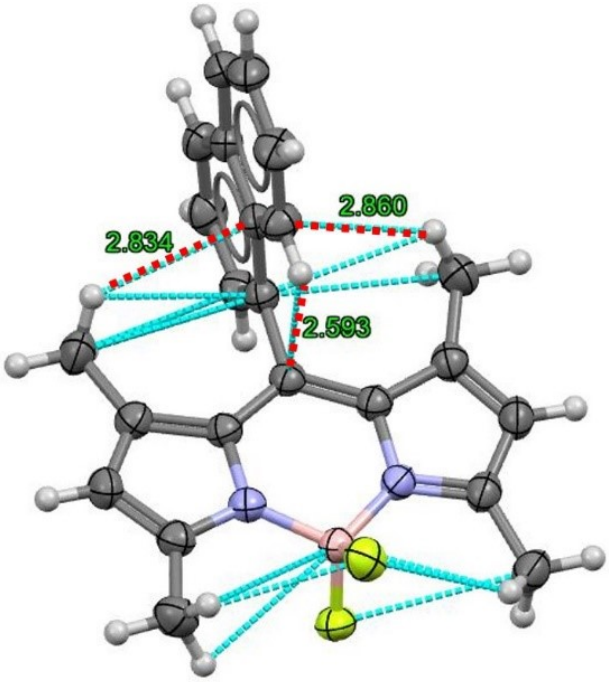

Figure S6. The illustration of intramolecular interactions of BDP-2 (Mercury, displaying options: intramolecular separated by > 3 bonds), in which red dotted lines are highlighted for extra contributions from the second benzene ring of naphthalene substituent.

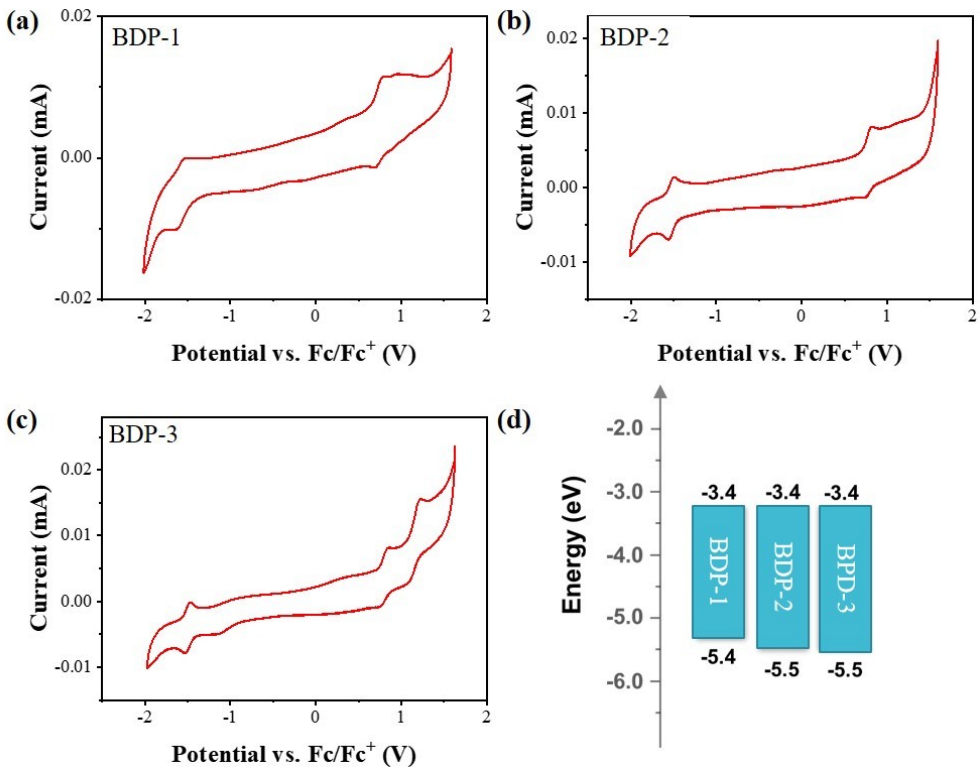

Figure S7. (a~c) The CV curves of BDP-1, BDP-2, and BDP-3 in acetonitrile. (d) energetic diagrams of HOMO-LUMO levels for BDP-1, BDP-2, and BDP-3, respectively.

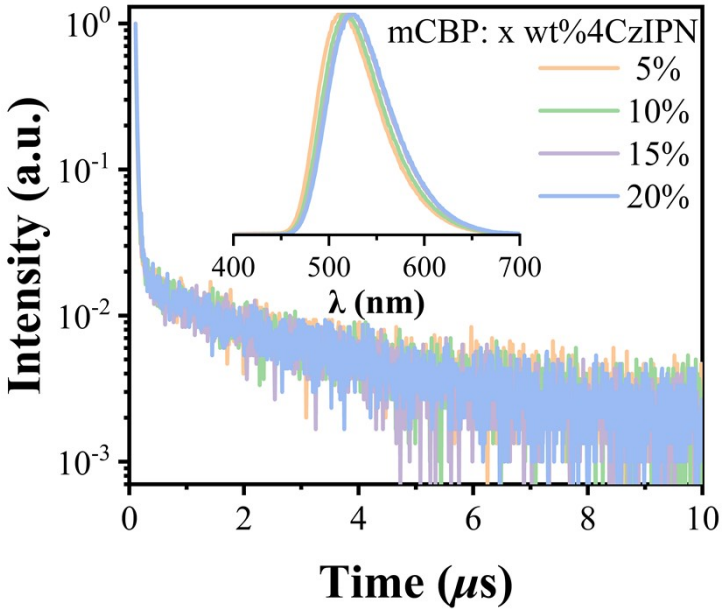

Figure S8. PL decay curves of films comprised of mCBP: x wt.% 4CzIPN (x: 5~20) (inset: steady-state PL spectra).

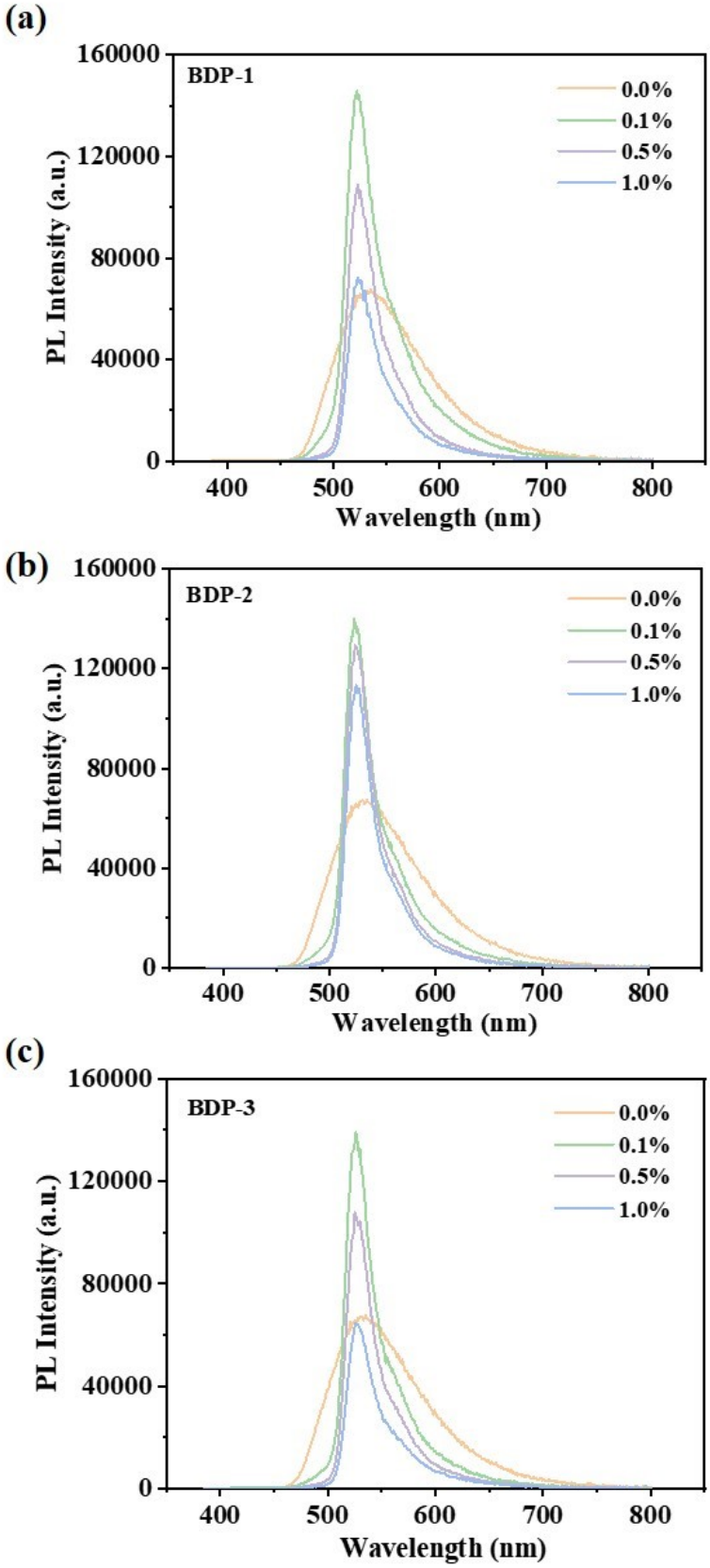

Figure S9. The emission spectra of films of mCBP: 20 wt% 4CzIPN: x wt% BDP-1 and BDP-3 (x: 0.0~1.0 wt%).

Table S1. The FET radius and FET efficiency are calculated under different doping ratios.

Matrix	Compound	R_0 (nm)	r (nm)	E_{FET} (%)
mCBP: 20 wt.% 4CzIPN	0.1 wt.% BDP-1	3.96	3.75	58
	0.5 wt.% BDP-1		2.79	89
	1.0 wt.% BDP-1		2.57	93
	0.1 wt.% BDP-2	4.07	3.48	72
	0.5 wt.% BDP-2		2.77	91
	1.0 wt.% BDP-2		2.57	94
	0.1 wt.% BDP-3	4.21	3.51	75
	0.5 wt. % BDP-3		2.74	93
	1.0 wt.% BDP-3		2.48	96

$$R_0 = 0.211(k^2 n^{-4} Q_D\, J(\lambda))^{1/6}$$

$$J = \int f_D(\lambda)\varepsilon_A(\lambda)(\lambda)^4 d(\lambda)$$

$$\mathbf{E_{FET}} = [1-(F_{DA}/F_D)]\times 100\%$$

$$E_{FET} = \frac{R_0^6}{R_0^6 + r^6}$$

in which $\mathbf{R_0}$ (Forster radius) is the distance at which the energy transfer efficiency is 50%. n is the refractive index (1.8), κ is the dipole orientation factor (k^2=0.67), Q_D is the prompt PLQY of the assistant host. **r** is the actual distance between energy donor, i.e. 4CzIPN, and the energy acceptor, i.e. BDP-1~3.[1]

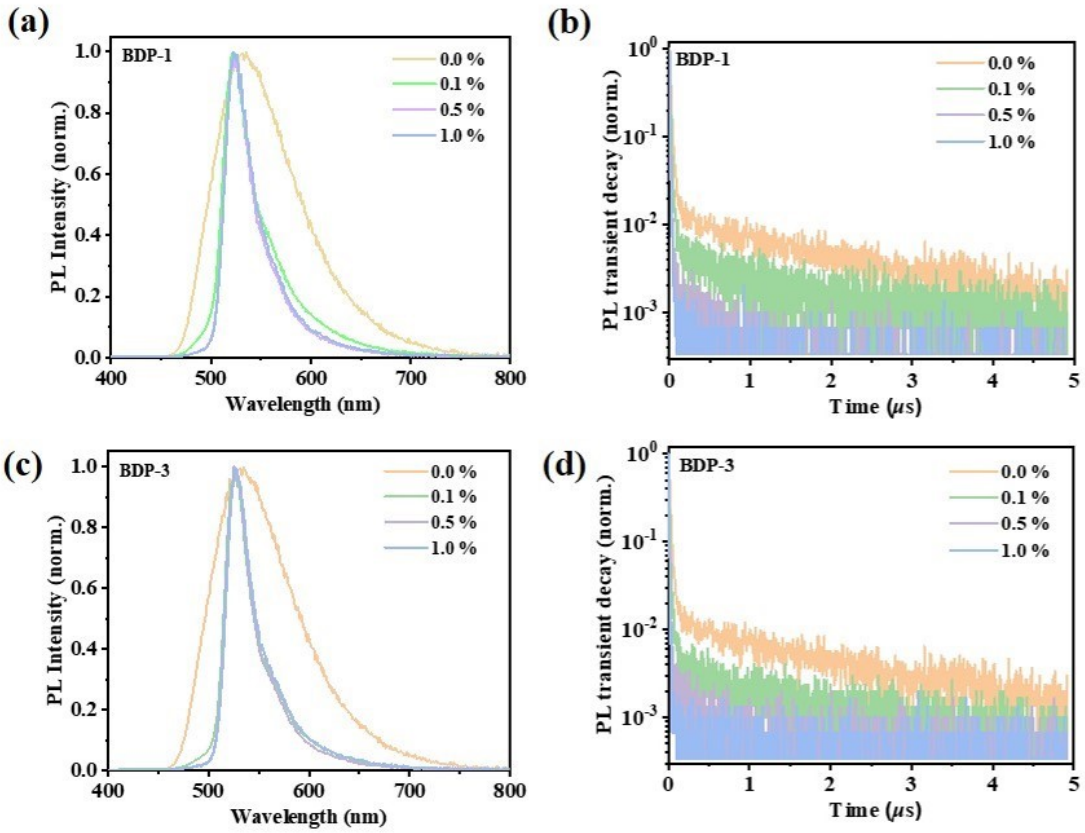

Figure S10. (a~d) The emission spectra and PL decay curves of films of mCBP: 20 wt% 4CzIPN: x wt% BDP-1 and BDP-3 (x: 0.0~1.0 wt%).

Table S2. PL characteristics and rate constants of mCBP: 20wt% 4CzIPN: x wt% BDP-1~3 films (0.0~1.0wt%)

Compound	λ_{PL} [nm]	FWHM [nm]	τ_{PF} [ns]	τ_{DF} [ns]	Φ_{PL} [%]	Φ_{PF} [%]	Φ_{DF} [%]	k_{ISC} [10^7 s^{-1}]	k_{RISC} [10^5 s^{-1}]
20% 4CzIPN	530	97.6	12.3	1734.5	41.5	13.62	27.88	7.02	13.66
0.1% BDP-1	521	35.1	9.5	398.5	51.7	34.50	17.20	7.02	13.66
0.5% BDP-1	524	33.5	5.3	17.8	46.7	43.93	2.77	7.02	13.66
1.0% BDP-1	526	33.0	4.6	8.9	40.4	40.36	0.04	7.02	13.66
0.1% BDP-2	523	30.4	10.1	185.4	65.9	49.10	16.80	7.02	13.66
0.5% BDP-2	526	30.2	5.2	17.3	58.9	55.59	3.31	7.02	13.66
1.0% BDP-2	526	29.8	4.1	9.9	52	51.07	0.93	7.02	13.66
0.1% BDP-3	525	30.2	9.4	417.2	45.1	30.84	14.26	7.02	13.66
0.5% BDP-3	527	31.0	5.6	31.4	37.4	33.67	3.73	7.02	13.66
1.0% BDP-3	528	30.2	4.8	10	33.7	32.09	1.61	7.02	13.66

The measurements were performed at room temperature and in vacuum, where k_{ISC} and k_{RISC} represent intersystem crossing and reverse intersystem crossing rates, respectively, by the method described by Masui et al[2].

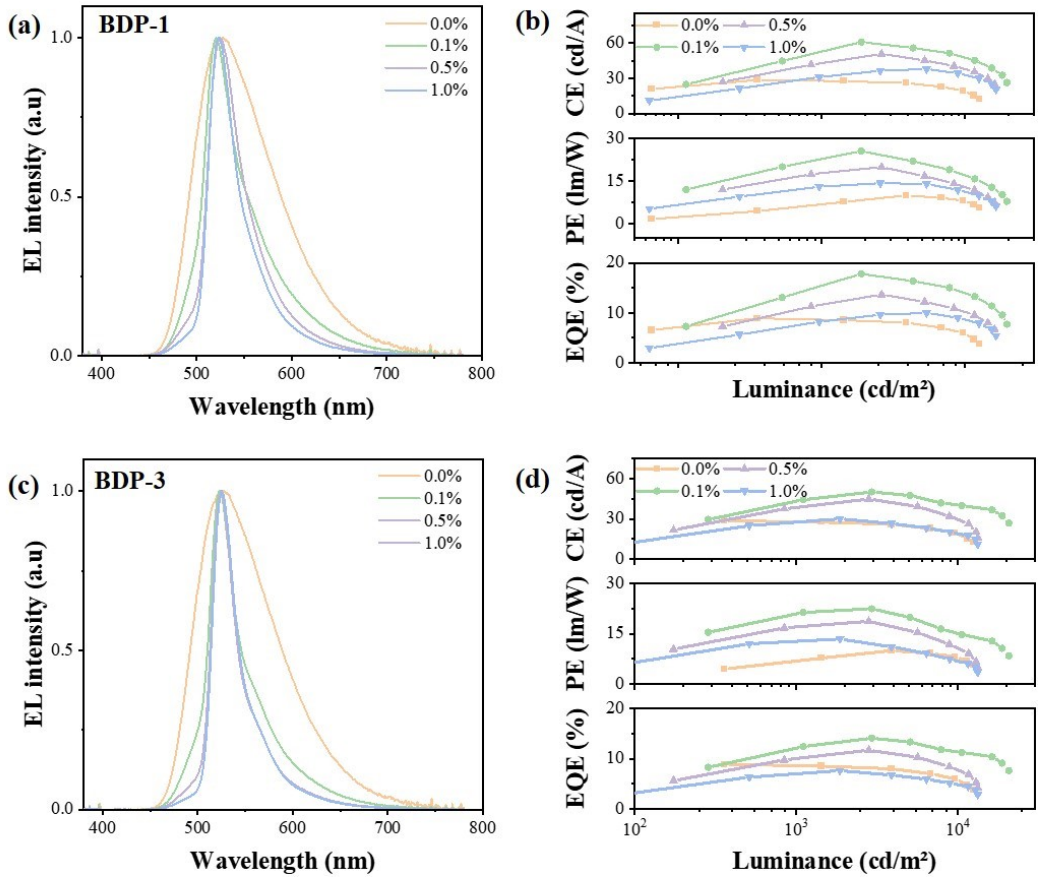

Figure S11. (a~d) The EL Spectrum and CE, PE, and EQE-L curves of the devices based on BDP-1 or BDP-3.

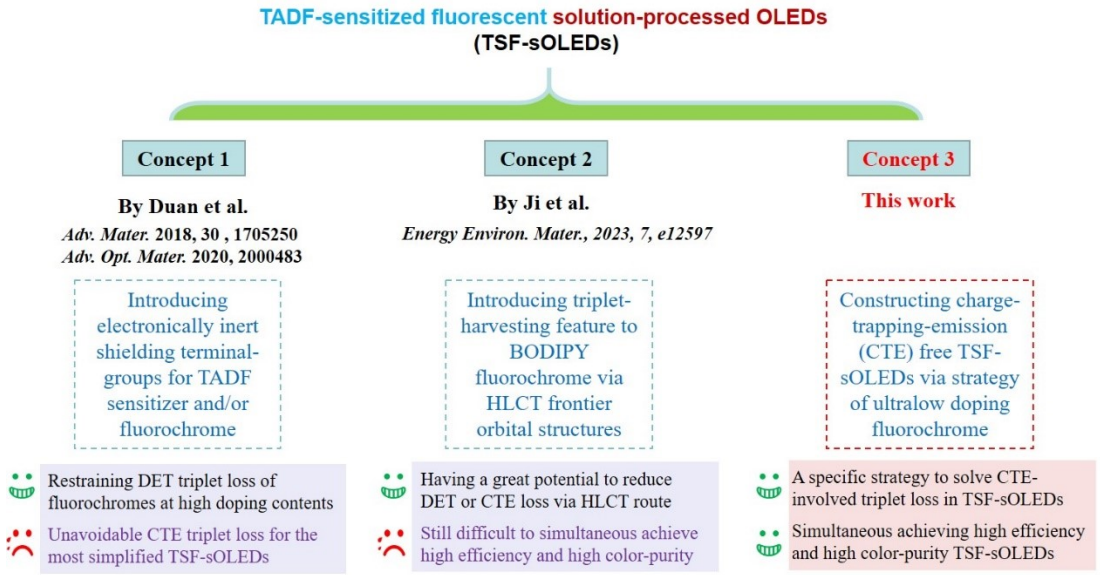

Figure S12. The comparisons of three concepts developed for TSF-sOLEDs.

Table S3. Roadmaps for the development of TSF-OLEDs based on BODIPY fluorochromes, including either solution-processed devices or thermal evaporation devices.

Device type	Concept	TADF sensitizer	Fluorochrome	EQE_{max} [%]	FWHM [nm]	CIE (x,y)	Reference
Solution Processed	3	4CzIPN	**BDP-2**	**21.5**	**31**	**(0.28, 0.65)**	**This work**
	2	4CzIPN	BDP-C-Cz	19.25	63	(0.57,0.41)	3
	2	4CzIPN	BDP-N-Cz	19.12	55	(0.52,0.47)	3
	1	phCz-4CzTPN	B1	1.5	49	(0.63, 0.37)	4
	1	phCz-4CzTPN	B2	1.9	51	(0.66, 0.34)	4
	1	phCz-4CzTPN	B3	1.0	52	(0.67, 0.33)	4
	1	phCz-4CzTPN	p-OMB	1.2	55	(0.64, 0.36)	5
	1	phCz-4CzTPN	o-OMB	0.7	68	(0.61,0.38)	5
	1	4CzIPN	Ph-2TPA	2.4	60	(0.64,0.36)	6
	1	4CzIPN	CF-2TPA	2.2	61	(0.63,0.36)	6
	1	4CzIPN	5tbuph-bodipy	4.9	47	(0.64,0.36)	7
Thermal Evaporation	1	4CzIPN	2CF-2TPA	2.3	63	(0.61,0.39)	6
	1	4CzIPN	tPhBODIPY	19.0	32	(0.26, 0.67)	8
	1	4CzIPN	tPhBODIPY	18.8	32	-	9
	1	4CzIPN	4tBuMB	19.4	44	(0.64, 0.36)	10
	1	NAI-DMAC	BF-PZ	13.3	37	(0.66,0.34)	11
	1	NAI-DMAC	MeBF-PZ	18.3	30	(0.67,0.33)	11
	1	NAI-DMAC	MeBF-MePZ	21.1	30	(0.62,0.38)	11

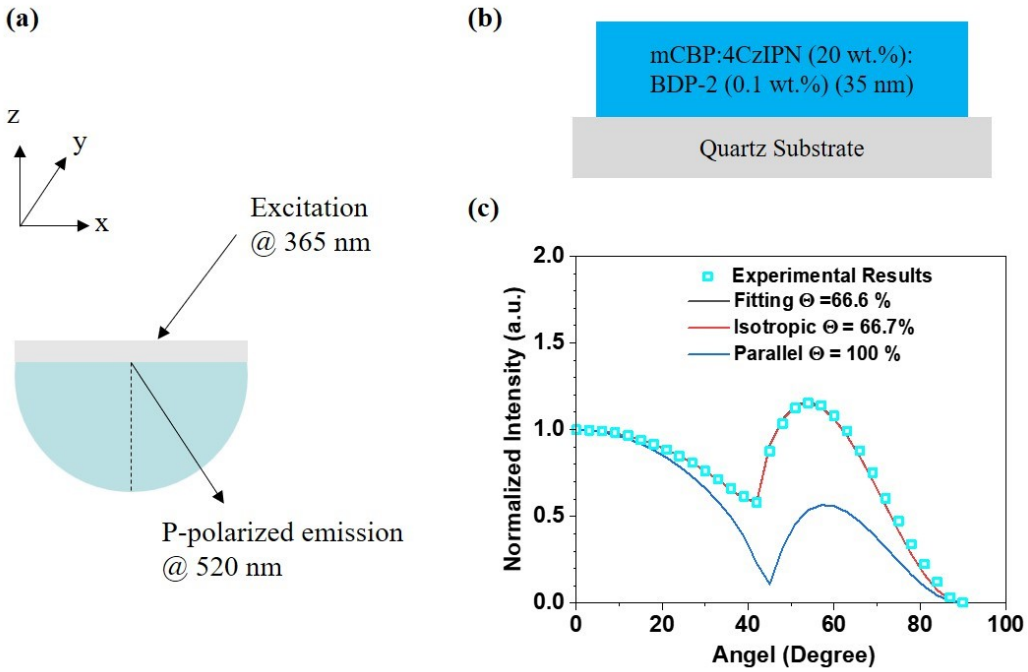

Figure S13. Schematic illustration of angle-dependent PL measurements (a), the corresponding film sample structure of mCBP:4CzIPN (20 wt.%):BDP-2 (0.1 wt.%) doped EML (b), the experimental testing and fitting results (c), respectively.

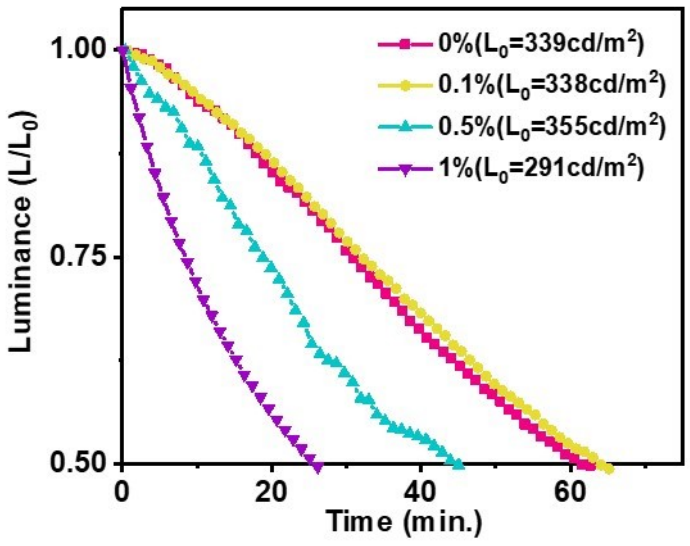

Figure S14. The comparisons of device lifetimes of TSF-sOLEDs using different doping concentrations of BDP-2.

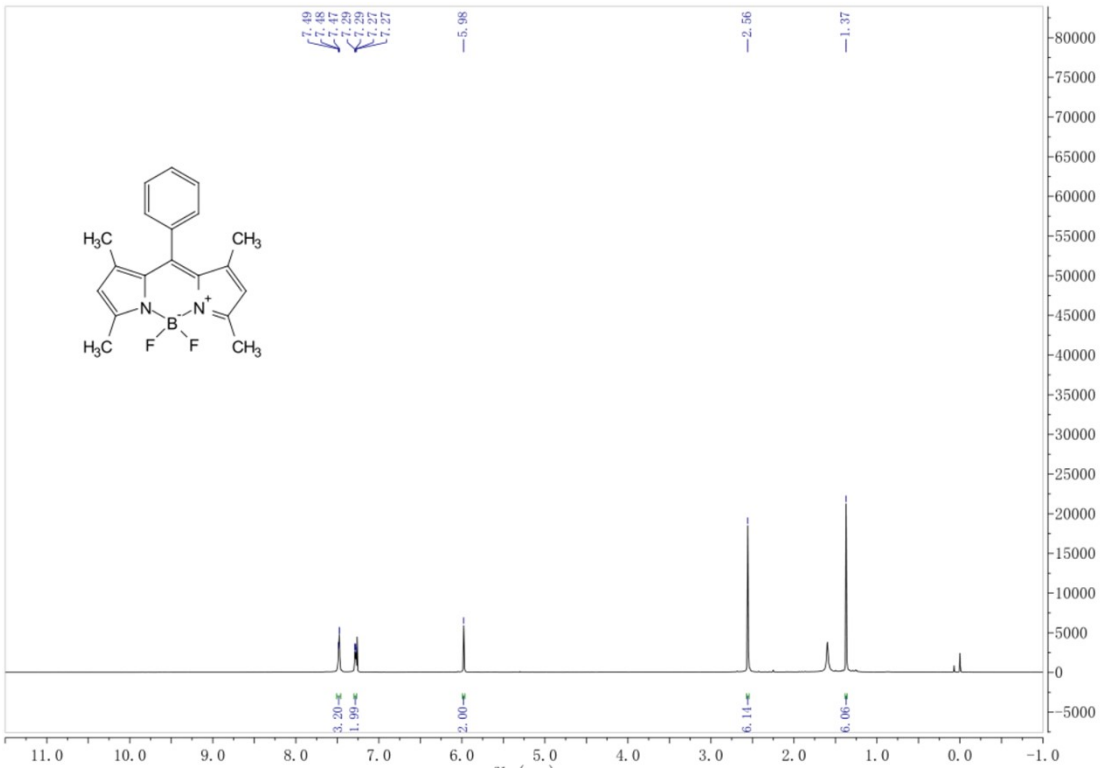

Figure S15. [1]H NMR spectra of BDP-1.

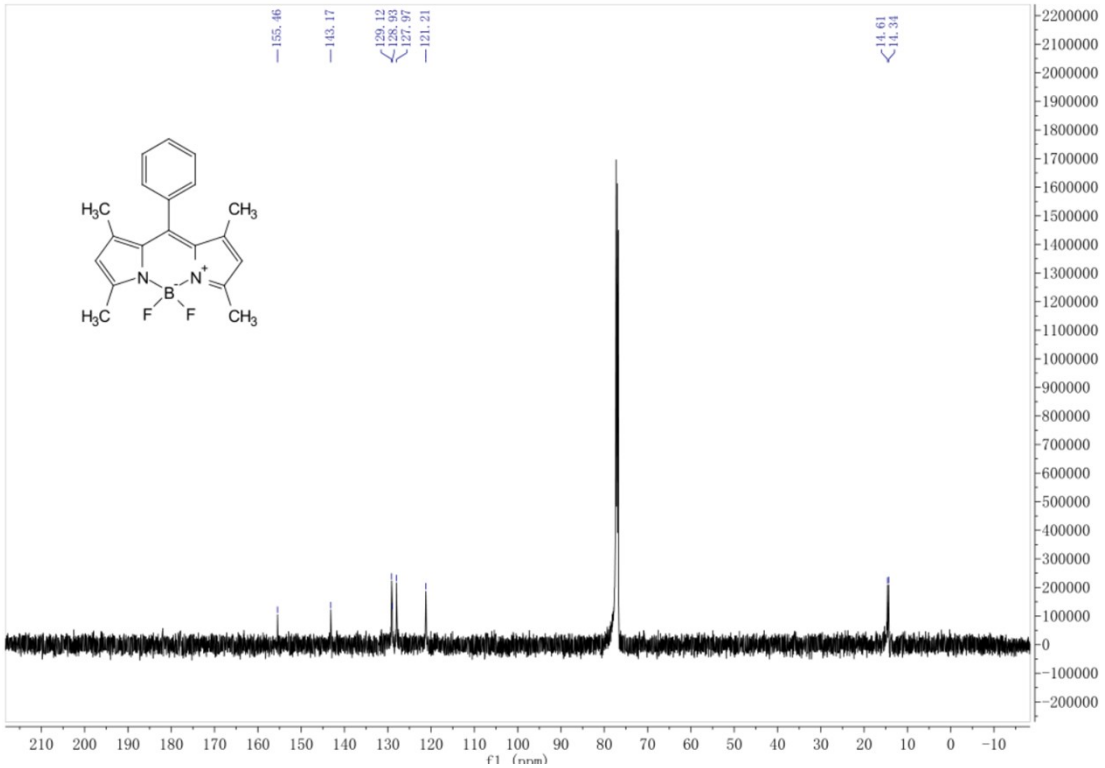

Figure S16. [13]C NMR spectra of BDP-1.

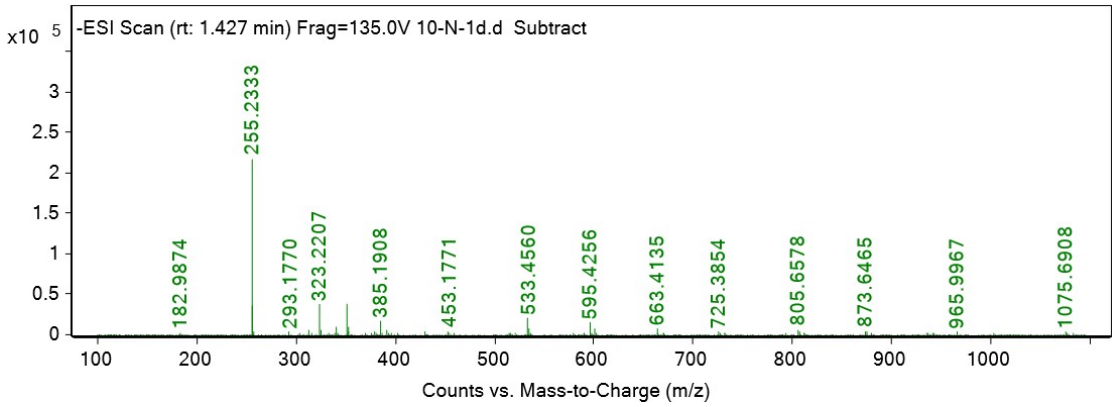

Figure S17. HRMS of BDP-1.

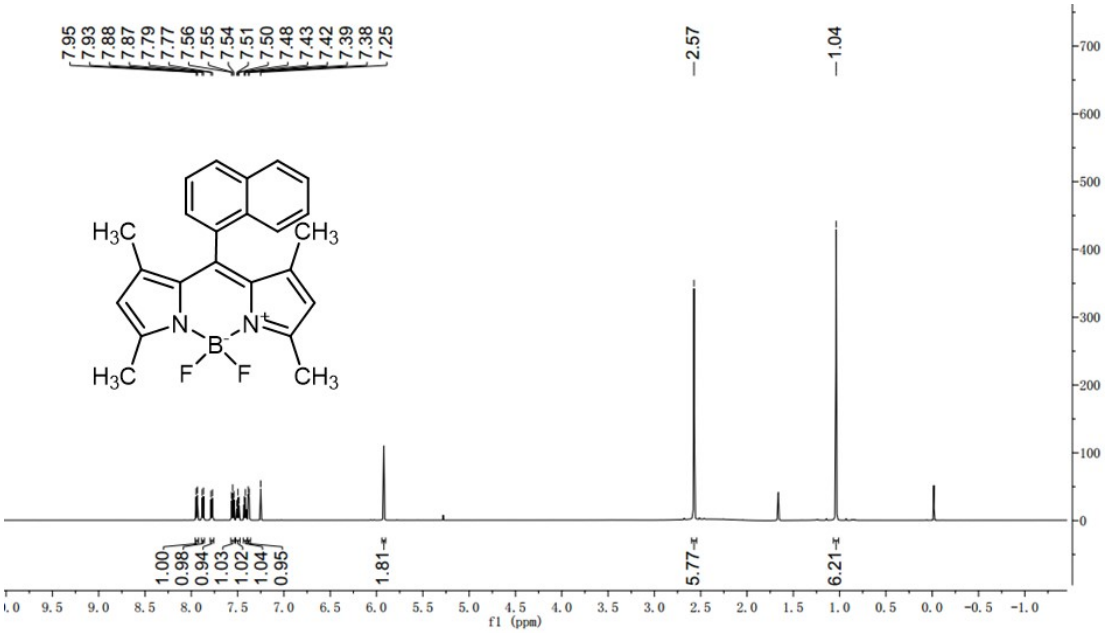

Figure S18. ^{1}H NMR spectra of BDP-2.

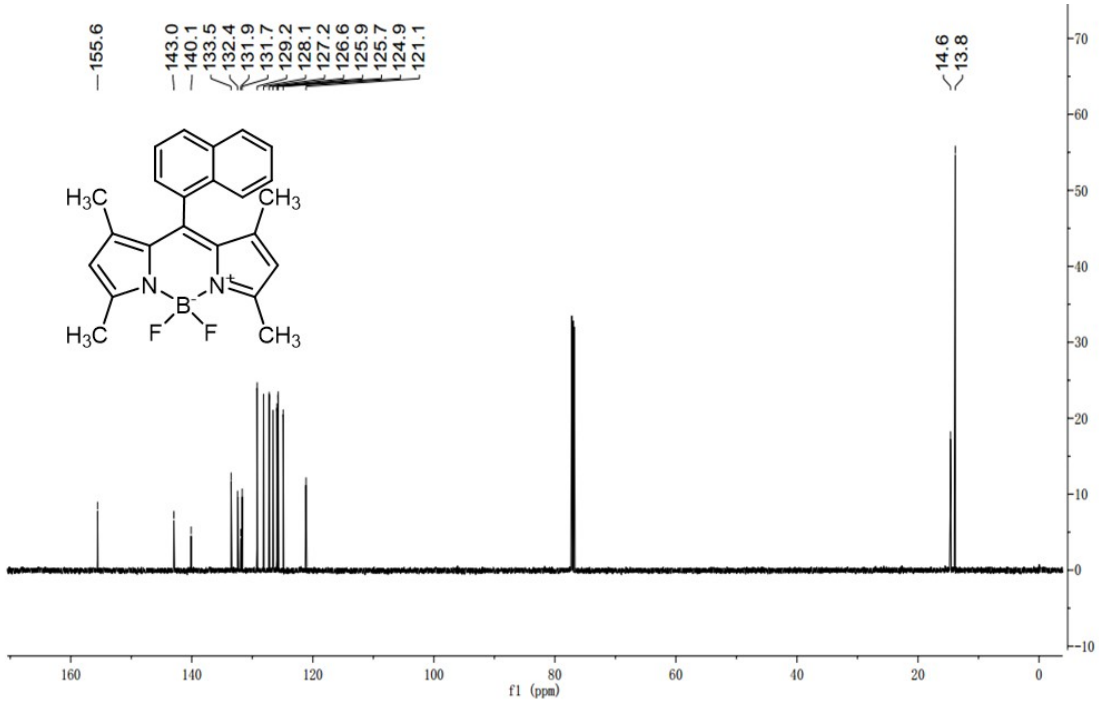

Figure S19. ^{13}C NMR spectra of BDP-2.

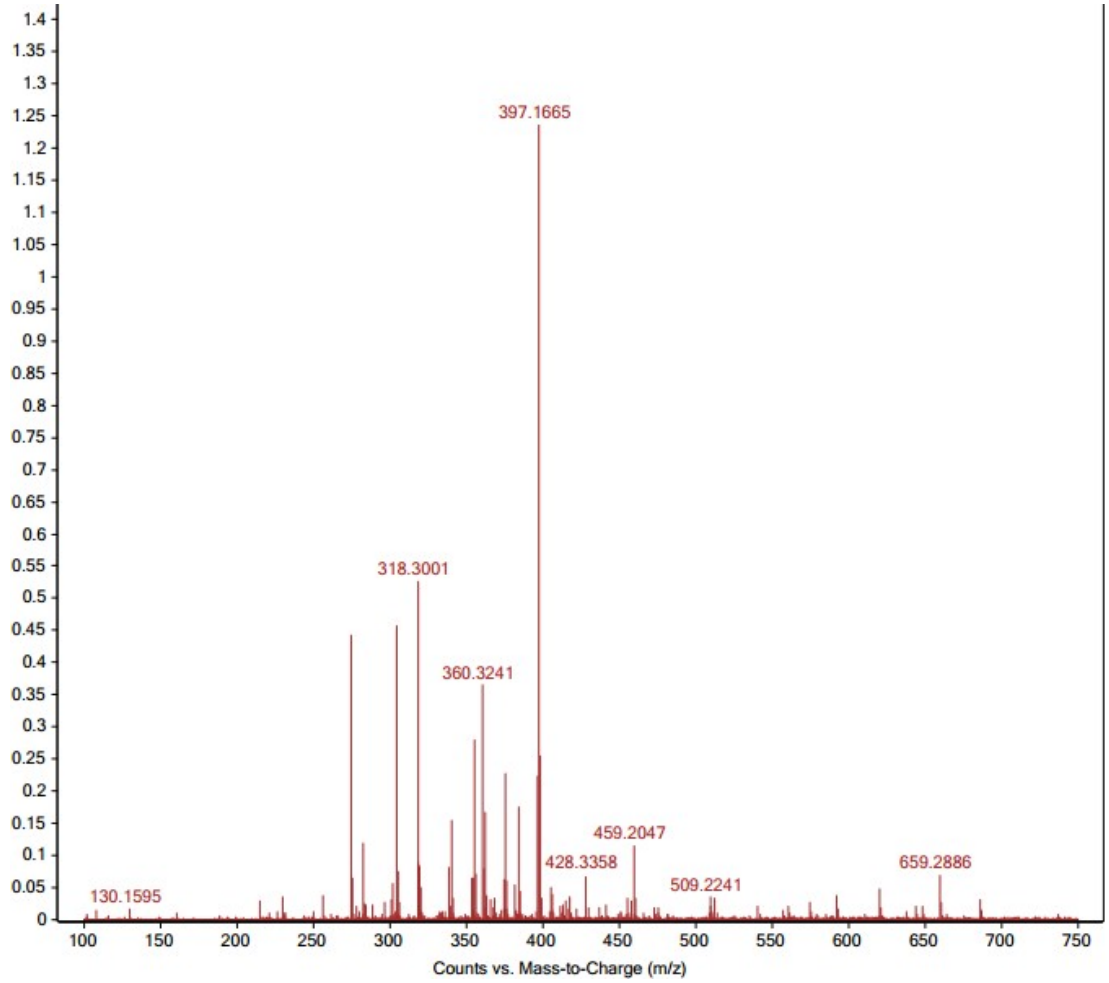

Figure S20. HRMS of BDP-2.

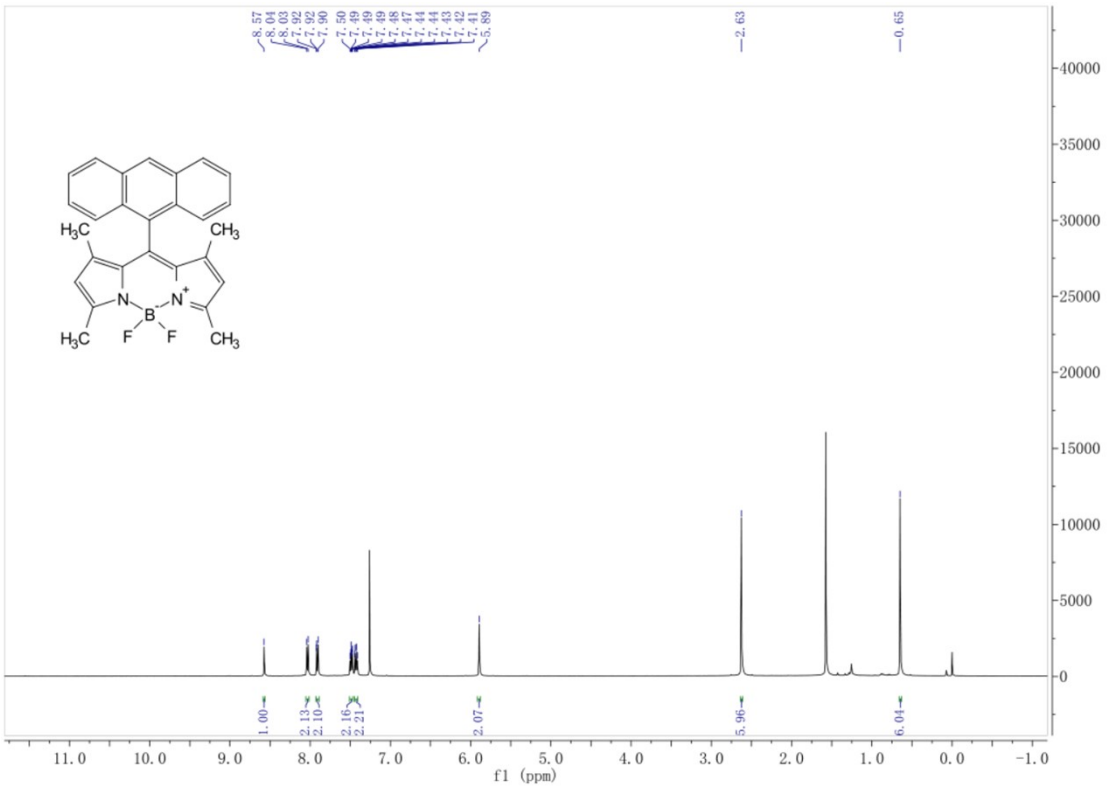

Figure S21. ^{1}H NMR spectra of BDP-3.

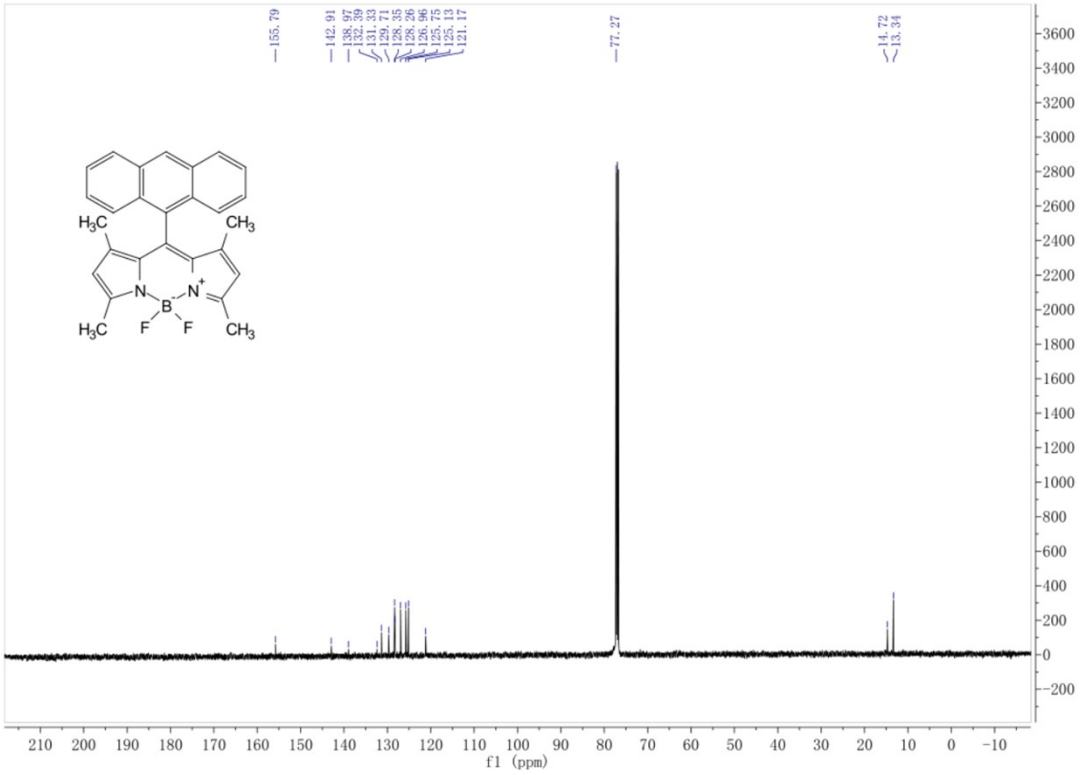

Figure S22. ^{13}C NMR spectra of BDP-3.

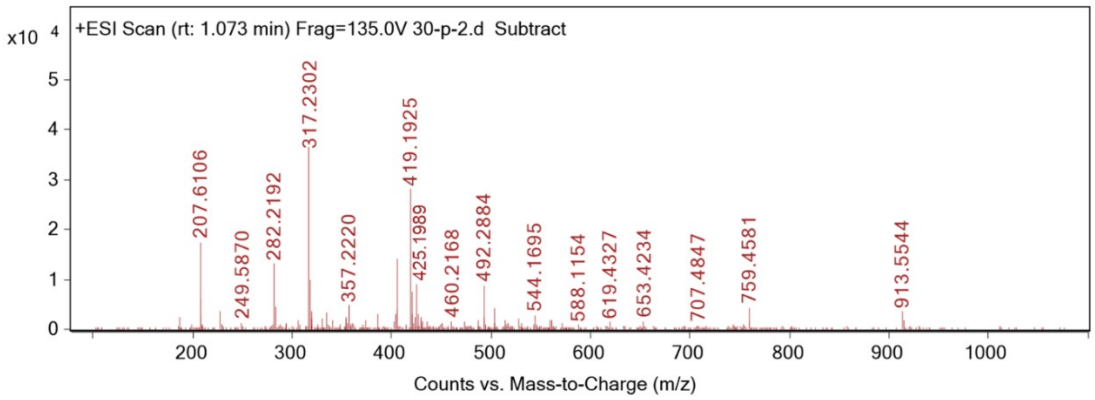

Figure S23. HRMS of BDP-3.

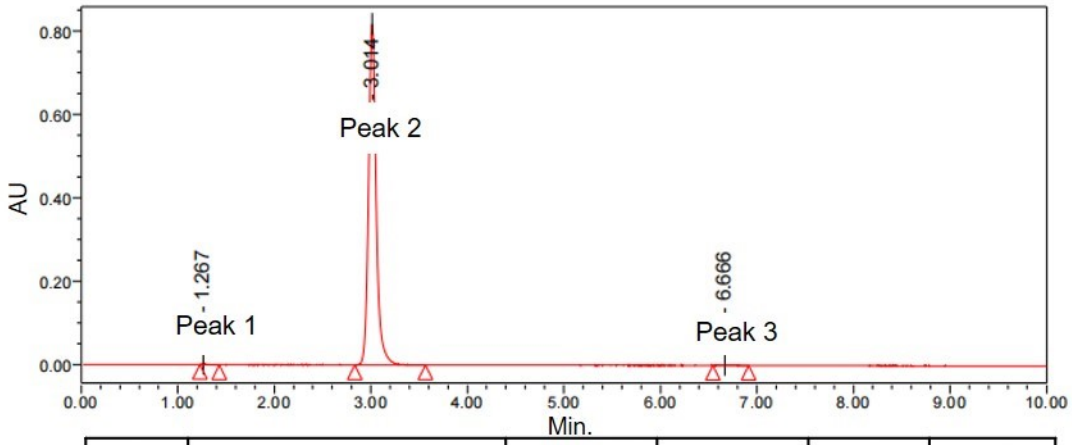

Peak No.	Processing channel	Retention time (min.)	area	% area	Peak Hight
1	PDA Ch1 500 nm@ 4.8 nm	1.267	8010	0.18	2499
2	PDA Ch1 500 nm@ 4.8 nm	3.014	4490356	99.54	818376
3	PDA Ch1 500 nm@ 4.8 nm	6.666	12571	0.28	1267

Figure S24. HLPC plot of BDP-1.

As measured, the HLCT purity of such sample is 99.54%.

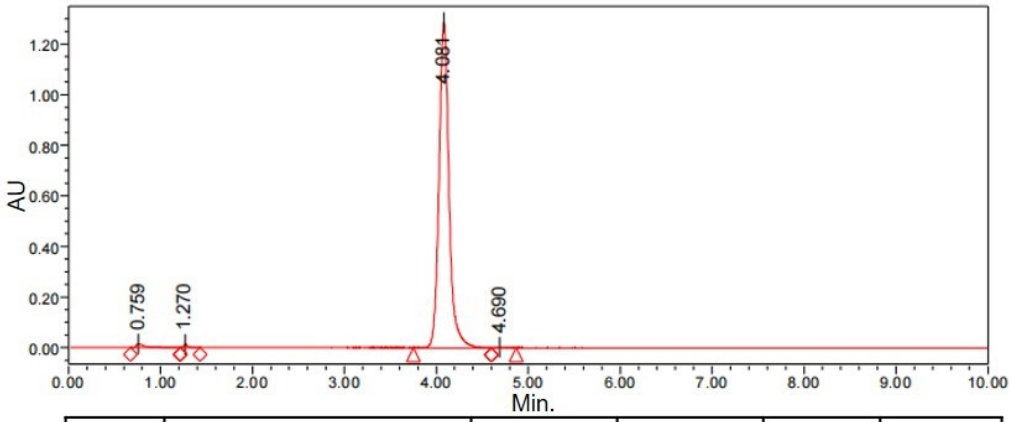

Peak No.	Processing channel	Retention time (min.)	area	% area	Peak Hight
1	PDA Ch1 500 nm@ 4.8 nm	0.759	106665	1.07	14960
2	PDA Ch1 500 nm@ 4.8 nm	1.270	39560	0.40	13234
3	PDA Ch1 500 nm@ 4.8 nm	4.081	9806115	98.41	1285374
4	PDA Ch1 500 nm@ 4.8 nm	4.690	11877	0.12	1508

Figure S25. HLPC plot of BDP-2.

As measured, the HLCT purity of such sample is 98.41%.

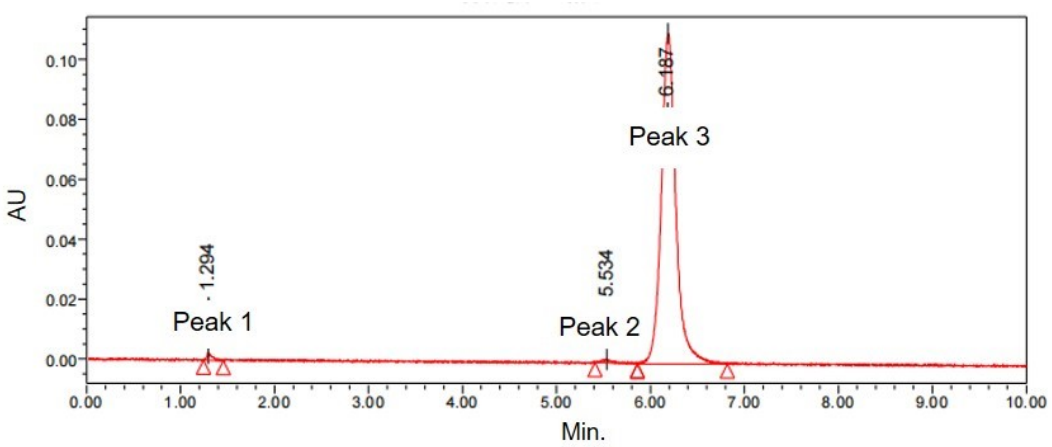

Peak No.	Processing channel	Retention time (min.)	area	% area	Peak Hight
1	PDA Ch1 500 nm@ 4.8 nm	1.294	9996	0.82	2390
2	PDA Ch1 500 nm@ 4.8 nm	5.534	12030	0.99	1168
3	PDA Ch1 500 nm@ 4.8 nm	6.187	1193310	98.19	110290

Figure S26. HLPC plot of BDP-3.

As measured, the HLCT purity of such sample is 98.19 %.

3. References

1. J. R. Lakowicz, *Principles of Fluorescence Spectroscopy*, Springer, University of Maryland School of Medicine Baltimore, Maryland,USA., 2008.
2. K. Masui, H. Nakanotani and C. Adachi, *Org. Electron.*, 2013, **14**, 2721-2726.
3 . X. W. Nie, Z. Mahmood, D. H. Liu, M. K. Li, D. H. Hu, W. C. Chen, L. J. Xing, S. J. Su, Y. P. Huo and S. M. Ji, *Energy. Environ. Mater.*, 2023, **7**, e12597.
4. D. Y. Ma, G. M. Zhao, H. W. Chen, R. Y. Zhou, G. H. Zhang, W. W. Tian, W. Jiang and Y. M. Sun, *Dyes and Pigments*, 2022, **203**, 110377.
5. W. Jiang, R. Zhou, G. Zhao, D. Ma, H. Chen, Z. Zhang, W. Tian and Y. Sun, *Opt. Mater.*, 2023, **136**, 113505.
6. G. M. Zhao, H. Y. Dai, R. Y. Zhou, G. H. Zhang, H. W. Chen, D. Y. Ma, W. W. Tian, X. X. Ban, W. Jiang and Y. M. Sun, *Org. Electron.*, 2022, **106**, 106530.
7. G. M. Zhao, R. Y. Zhou, G. H. Zhang, H. W. Chen, D. Y. Ma, W. W. Tian, W. Jiang and Y. M. Sun, *J. Mater. Chem. C*, 2022, **10**, 5230-5239.
8. Z. Song, D. D. Zhang, Y. W. Zhang, Y. Lu and L. Duan, *Adv. Opt. Mater.*, 2020, **8**, 2000483.
9. Nakamura, H. Sasabe, S. Abe, K. Kumada, R. Sugiyama, T. Hanayama and J. Kido, *Mol. Syst. Des. Eng.*, 2023, **8**, 866-873.
10. Y. H. Jung, D. Karthik, H. Lee, J. H. Maeng, K. J. Yang, S. Hwang and J. H. Kwon, *ACS Appl.Mater. nterfaces*, 2021, **13**, 17882-17891.
11. H. Liu, J. J. Liu, H. Y. Li, Z. Y. Bin and J. S. You, *Angew. Chem. Int. Ed.*, 2023, **62**, e202306471.